small NANO MICRO

Biosensors

Graphene Oxide-Based Fluorescent Biosensor for Protein Detection via Terminal Protection of Small-Molecule-Linked DNA

Yue He, Xiaojing Xing, Hongwu Tang, and Daiwen Pang*

Proteins play very important roles in almost all functions of life. The detection and quantification of proteins are necessary in molecular diagnostics as well as in biomedical research. Affinity ligands, such as monoclonal antibody and aptamer, are typically used for protein detection.[1] Aptamer-based ligands have advantages over antibodies, such as low molecular weight, simple and reproducible synthesis, thermal stability, reusability, and long-term stability.[2] Besides, aptamers are also superior to antibodies in terms of signal transduction because of the predictable and tailorable structures of nucleic acids.[3]

Although aptamers can bind a variety of targets with high selectivity and sensitivity, some proteins only have RNA aptamers that are unstable and easily degraded by ribonucleases, and aptamers of some proteins have not been screened out yet.[4] Oligonucleotides terminally tethered with protein-binding small molecules may represent an ideal option for the detection of these proteins. For the protein binding the small-molecule moiety offers DNA the capacity for selective capture of the target proteins, and the DNA part can be randomly coded, thus providing enormous capabilities for signal transduction.[5] Recently, Jiang's group has reported that protein binding to small molecules in DNA–small-molecule chimeras could protect the conjugated DNA from degradation by the 3′ single-strand-specific exonuclease I (Exo I).[6] This finding, which is called terminal protection, forms a basis for constructing sensitive biosensors for electrochemical detection of proteins.[7] However, these electrochemical strategies may suffer from the limitations of requiring deliberate modifications of electrode surfaces and careful control of assay conditions. To overcome these limitations, Jiang's group designed a novel label-free fluorescent biosensor using DNA intercalating dyes (SYBR Green I)[8] to report the recognition and binding between the small molecule at the terminus of the DNA strand and the target protein. Chen's group also developed a novel label-free fluorescent biosensor for folate receptor (FR) detection using quinaldine red as a G-quadruplex-binding probe.[9] These methods, although they have distinct advantages, also present their own limitations, such as high background and lack of multiplex detection capability. Therefore, it remains important to find new approaches that could overcome these problems.

Graphene, as a novel carbon nanomaterial, is a single-atom-thick, two-dimensional carbon material that has attracted great interest for its remarkable electronic, mechanical, and thermal properties.[10] Due to its peculiar electronic properties, the water-soluble derivative of graphene, graphene oxide (GO), is an excellent energy acceptor in resonance energy transfer, which makes fluorescence detection a promising application of graphene in sensing technology.[11] In addition, GO can interact noncovalently with single-stranded DNA (ssDNA) by π–π stacking interactions between nucleotide bases and GO, but hardly interacts with rigid double-stranded DNA (dsDNA).[12] Moreover, GO can protect DNA against enzymatic cleavage and enhance the intracellular stability of DNA, compared with free DNA probes.[13] These properties of GO form a basis for constructing sensitive, selective, rapid, and cost-effective biosensors for DNA detection.

In this work, based on terminal protection of small-molecule-linked DNA by target proteins and the GO-assisted DNA assay strategy, we have developed a novel fluorescence method for the detection of target proteins. FR, a highly selective biomarker that is overexpressed by many primary and metastatic cancers, is used as the model target. As shown in **Figure 1**, in the absence of FR, the folate-linked DNA (probe 1) is hydrolyzed into mononucleotides by Exo I in the 3′ to 5′ direction. Besides, the fluorescence of fluorescein amidite (FAM)-labeled DNA (probe 2) that is previously adsorbed on the surface of GO is completely quenched by GO. The system shows very low background. However, upon the addition of FR, the specific binding of FR to the small-molecule folate of probe 1 protects probe 1 from Exo I-catalyzed digestion. Consequently, the presence of the target

Dr. Y. He, Dr. X. J. Xing, Prof. H. W. Tang, Prof. D. W. Pang
Key Laboratory of Analytical Chemistry for Biology and Medicine (Ministry of Education)
College of Chemistry and Molecular Sciences
Research Center for Nanobiology and Nanomedicine (MOE 985 Innovative Platform)
Wuhan Institute of Biotechnology, and State Key Laboratory of Virology
Wuhan University
Wuhan 430072, PR China
E-mail: hwtang@whu.edu.cn

DOI: 10.1002/smll.201202739

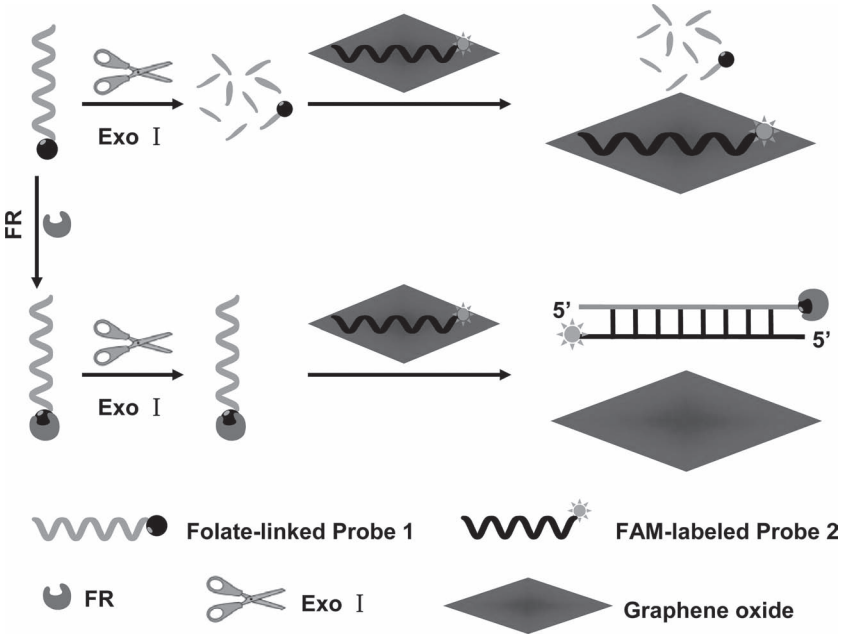

Figure 1. Scheme of the mechanism of a GO-based biosensor for folate receptor (FR) detection.

protein is translated into the appearance of residual probe 1 by Exo I-catalyzed DNA hydrolysis. After that, hybridization between the residual probe 1 and probe 2 occurs. Such hybridization will release probe 2 from the surface of GO, thereby resulting in the fluorescence restoration of FAM. Therefore, FR detection could be easily realized by monitoring the change of fluorescence signal.

To demonstrate the feasibility of this approach, the process of fluorescence quenching and restoration of this GO-based biosensor for FR detection is shown by fluorescence spectra. **Figure 2** shows the fluorescence emission spectra of FAM-labeled ssDNA (probe 2) under different conditions. The initial fluorescence from probe 2 (Figure 2, curve a) is significantly quenched to 1.5% of the original intensity in the presence of GO (curve b), thus indicating the strong adsorption of probe 2 on GO and the high fluorescence quenching efficiency of GO. Upon the addition of the complementary sequence of probe 2, probe 1, the quenched fluorescence is recovered to 61% of the original intensity (curve c). The fluorescence of the complex of probe 2–GO is, however, scarcely influenced by the addition of the mixture of probe 1 and Exo I (curve d), which means that the mononucleotides produced by Exo I-assisted hydrolyzation of probe 1 cannot recover the quenched fluorescence. Upon the addition of the mixture of target protein FR, probe 1, and Exo I, the fluorescence of the complex of probe 2–GO recovered significantly (curve d), thus implying that the specific binding of FR to the small-molecule folate of probe 1 protects probe 1 from Exo I-catalyzed digestion. These observations confirm that terminal protection of small-molecule-linked DNA by target protein and the GO-assisted DNA assay strategy could be used for the detection of FR.

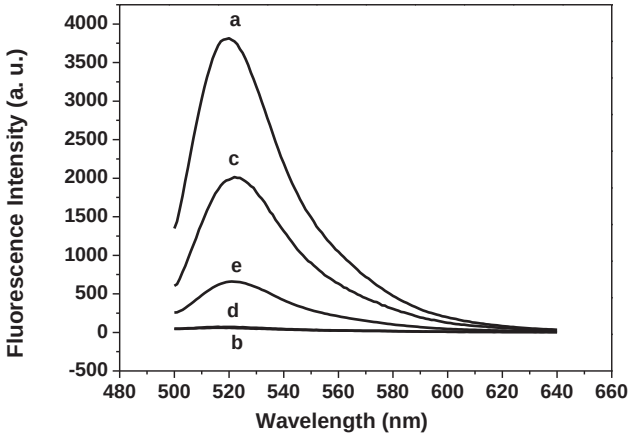

Figure 2. Fluorescence emission spectra of FAM-labeled ssDNA (probe 2) under different conditions: a) probe 2 in Tris-HCl buffer; b) probe 2 + GO; c) probe 2 + GO + probe 1; d) probe 2 + GO + (probe 1 + Exo I); e) probe 2 + GO + (probe 1 + FR + Exo I). Probe 1, 200 nM; probe 2, 50 nM; GO, 20 μg mL^{-1}; Exo I, 4 U. Excitation: 480 nm.

To achieve the best sensing performance, the concentration of GO was optimized (Supporting Information (SI), Figure S2). The fluorescence intensity of FAM-labeled probe 2 decreases sharply as the concentration of GO increases from 0 to 50 μg mL^{-1}. When the GO concentration is up to 20 μg mL^{-1}, the fluorescence intensity of FAM is quenched down to 1.5% of the original fluorescence signal. As a result, 20 μg mL^{-1} was taken as the optimized concentration for GO. The kinetic behaviors of probe 2 and GO, as well as the probe 2–GO complex with probe 1, were studied by monitoring the fluorescence intensity as a function of time (SI, Figure S3). Figure S3, curve a, shows the fluorescence quenching of probe 2 in the presence of GO as a function of incubation time. The adsorption of ssDNA on the surface of GO is very fast at room temperature. It reaches equilibrium in 5 min. However, the formation and release of the dsDNA from GO is relatively slow, and reaches equilibrium after 30 min (SI, Figure S3, curve b).

The concentration of Exo I and the Exo I-catalyzed digestion reaction time were optimized by measuring the fluorescence emission spectra of probe 2 and monitoring the fluorescence intensity of probe 2 as a function of time. As shown in Figure S4 (SI), the fluorescence intensity of FAM-labeled probe 2 decreases sharply as the concentration of Exo I increases from 0 to 10 U. When the Exo I concentration is up to 4 U, the fluorescence intensity of FAM is quenched down to 1.8% of the original fluorescence signal. As a result, 4 U was taken as the optimized concentration for Exo I. Figure S5 (SI) indicates the reaction time between probe 1 and Exo I, which is completed in about 30 min at 37 °C.

The assay of FR was carried out with fixed concentrations of probe 1 (200 nM), probe 2 (50 nM), GO (20 μg mL^{-1}),

small NANO MICRO

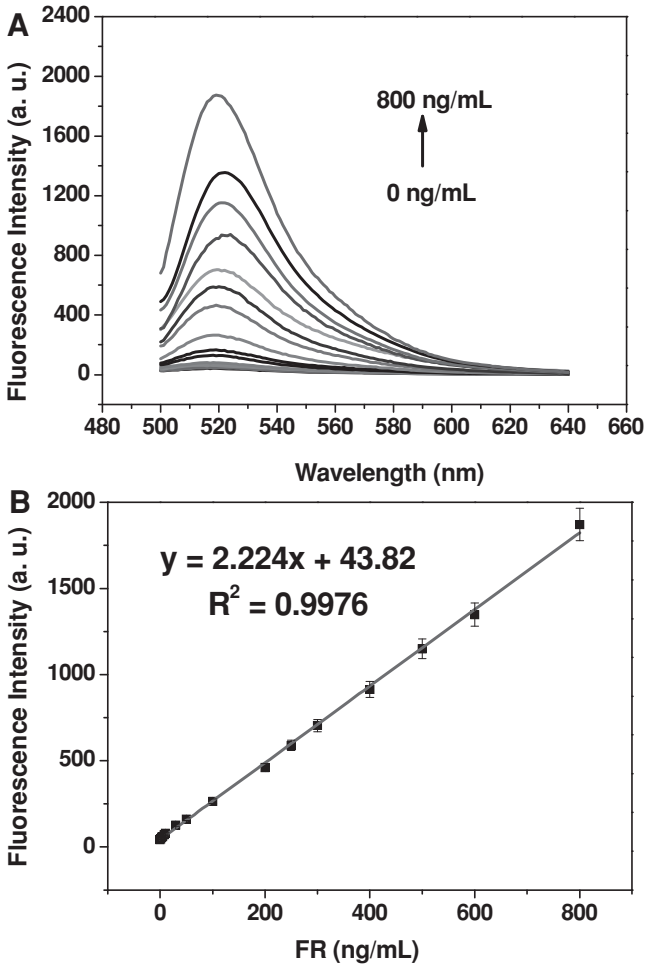

Figure 3. A) Fluorescence emission spectra of the GO-based biosensor upon the addition of increasing concentrations of FR. B) Calibration curve for FR detection. Probe 1, 200 nM; probe 2, 50 nM; Exo I, 4 U; GO, 20 μg mL^{-1}. Excitation: 480 nm.

and Exo I (4 U). **Figure 3**A shows the fluorescence emission spectra of the biosensor in the presence of different concentrations of FR. The fluorescence intensity of the sensor increases dramatically with the increasing concentration of FR. The calibration curve for FR detection is shown in Figure 3B, and the linear range is from 1 to 800 ng mL^{-1} with linear equation $y = 2.224x + 43.82$, where y is the fluorescence intensity of FAM at 520 nm and x is the concentration of FR (regression coefficient $R2 = 0.9976$). The detection limit is estimated to be 0.77 ng mL^{-1} ($3S_0/S$, in which S_0 is the standard deviation for the blank solution, $n = 11$, and S is the slope of the calibration curve), which is comparable to that of the electrochemical assay.[6,7] For each concentration of the protein, the measurement was repeated at least three times independently. The average relative standard deviation (RSD) is 1.18%, which indicates that the precision and reproducibility of the method are acceptable.

Additional assays were performed to inspect the selectivity of the assay to other samples. Under the optimized detection conditions, bovine serum albumin (BSA), thrombin, and streptavidin (SA) were selected to study the specificity

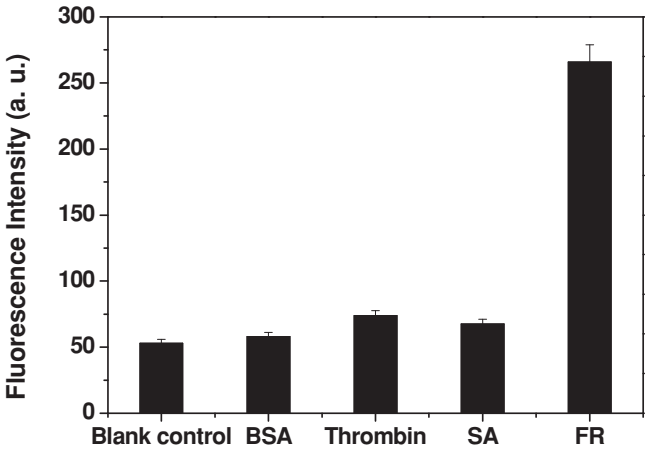

Figure 4. Fluorescence intensity of the GO-based biosensor in the presence of different proteins: blank control (without FR), BSA (100 ng mL^{-1}), thrombin (100 ng mL^{-1}), SA (100 ng mL^{-1}), and FR (100 ng mL^{-1}). Excitation: 480 nm.

of this GO-based biosensor. In a typical experiment, the biosensor was incubated with BSA, thrombin, SA, or FR (each 100 ng mL^{-1}). As shown in **Figure 4**, the fluorescence of this GO-based biosensor changed less for BSA, thrombin, and SA, whereas a significant fluorescence increase was observed for FR. The good selectivity of the biosensor is attributed to the high specificity between folate and FR. Therefore, this GO-based biosensor can be applied in highly sensitive detection of FR with high specificity.

Furthermore, to confirm the practicability for real sample analysis, we applied the above GO-based biosensor to FR detection in serum. The interaction between GO and FAM-labeled probe 2 in 2% serum was examined as outlined above, and 200 μg mL^{-1} was taken as the optimized concentration for GO (SI, Figure S6). The detection process of FR in 2% serum was the same as in the Tris-HCl buffer. As shown in Figure S7 (SI), there is still a good linear relationship between the fluorescence intensity and the concentration of FR. This clearly shows that the GO-based biosensor can be used to detect FR in practical samples sensitively. However, the change of fluorescence intensity is much smaller in serum assay compared with that in Tris-HCl buffer assay, which maybe attributed to the strong light-scattering effect of serum.[14]

To further confirm the generality of our design, we also used this method to detect SA by simply changing the small-molecule moiety of probe 1 to biotin, which we call probe 3. As shown in Figure S8 (SI), there is a good linear relationship between the fluorescence intensity and the concentration of SA as well. This clearly shows that the GO-based biosensor can be used to detect other proteins by simply changing the small molecule at the terminus of DNA.

In conclusion, a simple, selective, and sensitive fluorescent biosensor for FR detection based on terminal protection of small-molecule-linked DNA by target proteins and a GO-assisted DNA assay strategy was developed. This method generally converts small-molecule–protein interaction assays into the detection of DNA, which shows extraordinary sensitivity for FR detection in both buffer and serum. For FR, a

detection limit of 0.77 ng mL^{-1} was obtained. On the basis of this excellent performance, the generalized terminal protection mechanism and the GO-assisted strategies for the protein–small-molecule interaction assay were expected to hold considerable potential for molecular diagnostics, genomic research, and drug development.

Experimental Section

Apparatus: Fluorescence emission spectroscopy was performed on an F-4600 fluorescence spectrophotometer (Hitachi High-Technology Co., Ltd., Tokyo, Japan). The sample cell was a 700 μL quartz cuvette. The luminescence intensity was monitored by exciting the sample at 480 nm and measuring the emission at 520 nm. The slits for excitation and emission were set at 5 and 10 nm, respectively. The fitting of the experimental data was accomplished by using the software Origin 8.0.

Materials: Probe 1 used in this work was synthesized by Takara Biotechnology Co., Ltd. (Dalian, China). The sequence is as follows: 5′-AATACCACATCATCCATATA-folate-3′ (probe 1). The oligonucleotides probe 2 and probe 3 were synthesized by Sangon Biotechnology Co., Ltd. (Shanghai, China). Their sequences are as follows: 5′-TATATGGATGATGTGGTATT-FAM-3′ (probe 2) and 5′-AATACCACATCATCCATATA-biotin-3′ (probe 3). Graphene oxide (GO) was purchased from Sinocarbon Materials Technology Co., Ltd. (China). Exonuclease I (Exo I) was purchased from Takara Biotechnology Co., Ltd. (Dalian, China). The buffer solutions used were as follows: Exo I buffer consisted of 67 mM glycine–KOH (pH 9.5), 1 mM dithiothreitol (DTT), and 6.7 mM $MgCl_2$, and the Tris-HCl buffer consisted of 20 mM Tris-HCl (pH 7.4), 5 mM $MgCl_2$, and 50 mM NaCl. Milli-Q purified water was used to prepare all the solutions.

Optimization of the Concentration of GO: The purchased GO[15] was sonicated in Milli-Q purified water for 5 h to give a homogeneous black solution and stored at 4°C for use. The characterization of the purchased GO was performed and the results are shown in Figure S1 (SI). The working solution containing probe 2 was obtained by diluting the stock solution to a concentration of 50 nM with 20 mM Tris-HCl buffer.

To optimize the concentration of GO, 25 μL probe 2 (1 μM) and 0, 5, 10, 20, 30, 40, or 50 μL GO solution (500 μg mL^{-1}) as prepared were mixed. The mixed solution was diluted with Tris-HCl buffer to 500 μL, then incubated for 10 min at room temperature. Finally, the fluorescence intensity of the incubated solution was measured at 520 nm with excitation at 480 nm.

Optimization of the Reaction Time between Probe 2 and GO, as well as Probe 2–GO Complex with Probe 1: To optimize the reaction time between probe 2 and GO, probe 2 (25 μL, 1 μM) and GO (20 μL, 500 μg mL^{-1}) solutions were mixed. The mixed solution was diluted with Tris-HCl buffer to 500 μL and incubated for 0, 1, 5, 10, 20, and 30 min at room temperature. Finally, the fluorescence intensity of the incubated solution was measured at 520 nm with excitation at 480 nm.

To optimize the reaction time between probe 2–GO complex and probe 1, probe 2 (25 μL,1 μM) and GO (20 μL, 500 μg mL^{-1}) solutions were mixed. The mixed solution was incubated for 10 min at room temperature. Then probe 1 (10 μL, 10 μM) was added to the above solution, diluted with Tris-HCl buffer to 500 μL, and incubated for 0, 1, 5, 10, 20, and 30 min at room temperature. Finally, the fluorescence intensity of the incubated solution was measured at 520 nm with excitation at 480 nm.

Optimization of the Concentration of Exo I: To optimize the concentration of Exo I, we first prepared the probe 2–GO complex solution by adding probe 2 (25 μL, 1 μM) to GO (20 μL, 500 μg mL^{-1}) solution and incubating for 10 min at room temperature. To optimize the concentration of Exo I, 10 μL probe 1 (10 μM) and 0, 1, 2, 4, 6, 8, and 10 U Exo I solution were mixed and incubated for 30 min at 37°C with gentle shaking. Then the solution was added to the probe 2–GO complex solution, diluted with Tris-HCl buffer to 500 μL, and incubated for 30 min at room temperature. Finally, the fluorescence intensity of the incubated solution was measured at 520 nm with excitation at 480 nm.

Optimization of the Reaction Time between Probe 1 and Exo I: To optimize the reaction time between probe 1 and Exo I, probe 1 (10 μL, 10 μM) and Exo I (4 U) solutions were mixed. This solution was incubated for 0, 5, 10, 20, 30, 40, and 60 min at 37 °C with gentle shaking. Then the solution was added to the probe 2–GO complex solution, diluted with Tris-HCl buffer to 500 μL, and incubated for 30 min at room temperature. Finally, the fluorescence intensity of the incubated solution was measured at 520 nm with excitation at 480 nm.

Performance of FR Detection: For quantitative measurement of FR, probe 2 (25 μL, 1 μM) and GO (20 μL, 500 μg mL^{-1}) solutions were mixed and allowed to incubate for 10 min. A fixed concentration of probe 1 (200 nM) was treated with different concentrations of FR (0, 1, 3, 5, 7, 10, 30, 50, 100, 200, 250, 300, 400, 500, 600, and 800 ng mL^{-1}) and shaken gently for 1 h at 37 °C. After that, Exo I (4 U) was added to the solution, and the mixed solution was incubated for 30 min at 37 °C. Finally, the above mixture was added to the probe 2–GO complex and incubated for 30 min with gentle shaking at room temperature. Then the fluorescence intensity was measured at 520 nm with excitation at 480 nm.

Supporting Information

Supporting Information is available from the Wiley Online Library or from the author.

Acknowledgements

This work was supported by the National Basic Research Program of China (973 Program, Nos. 2011CB933600 and 2006CB933100), the Science Fund for Creative Research Groups of NSFC (Nos. 20621502 and 20921062), the National Natural Science Foundation of China (21275110, 20833006, 20875071, 21005056), and the Fundamental Research Funds for the Central Universities (20100141110015).

[1] a) R. F. Zuk, G. L. Rowley, E. F. Ullman, *Clin. Chem.* **1979**, *25*, 1554; b) Z. S. Wu, S. B. Zhang, H. Zhou, G. L. Shen, R. Q. Yu, *Anal. Chem.* **2010**, *82*, 2221.

[2] a) J. W. Liu, Z. H. Cao, Y. Lu, *Chem. Rev.* **2009**, *109*, 1948; b) M. Famulok, J. S. Hartig, G. Mayer, *Chem. Rev.* **2007**, *107*, 3715.

[3] S. D. Jayasena, *Clin. Chem.* **1999**, *45*, 1628.
[4] a) Y. J. Lee, S. W. Lee, *Biochem. Biophys. Res. Commun.* **2012**, *417*, 521; b) S. E. Lupold, B. J. Hicke, Y. Lin, D. S. Coffey, *Cancer Res.* **2002**, *62*, 4029.
[5] a) K. J. Cash, F. Ricci, K. W. Plaxco, *J. Am. Chem. Soc.* **2009**, *131*, 6955; b) Z. Zhen, L. J. Tang, J. Lin, J. H. Jiang, R. Q. Yu, X. L. Xiong, W. H. Tan, *Anal. Chem.* **2012**, *84*, 5708.
[6] Z. Wu, Z. Zhen, J. H. Jiang, G. L. Shen, R. Q. Yu, *J. Am. Chem. Soc.* **2009**, *131*, 12325.
[7] Y. Cao, S. Zhu, J. C. Yu, X. J. Zhu, Y. M. Yin, G. X. Li, *Anal. Chem.* **2012**, *84*, 4314.
[8] Z. Wu, H. Q. Wang, M. Guo, L. J. Tang, R. Q. Yu, J. H. Jiang, *Anal. Chem.* **2011**, *83*, 3104.
[9] X. F. Wei, W. L. Lin, N. Ma, F. Luo, Z. Y. Lin, L. H. Guo, B. Qiu, G. N. Chen, *Chem. Commun.* **2012**, *48*, 6184.
[10] a) K. S. Novoselov, A. K. Geim, S. V. Morozov, D. Jiang, Y. Zhang, S. V. Dubonos, I. V. Grigorieva, A. A. Firsov, *Science* **2004**, *306*, 666; b) A. K. Geim, K. S. Novoselov, *Nat. Mater.* **2007**, *6*, 183.
[11] a) R. S. Swathi, K. L. Sebastian, *J. Chem. Phys.* **2008**, *129*, 054703; b) R. S. Swathi, K. L. Sebastian, *J. Chem. Phys.* **2009**, *130*, 086101.
[12] a) Y. Wang, Z. H. Li, D. H. Hu, C. T. Lin, J. H. Li, Y. H. Lin, *J. Am. Chem. Soc.* **2010**, *132*, 9274; b) Y. Q. Wen, F. F. Xing, S. J. He, S. P. Song, L. H. Wang, Y. T. Long, D. Li, C. H. Fan, *Chem. Commun.* **2010**, *46*, 2596; c) C. L. Zhang, Y. X. Yuan, S. M. Zhang, Y. H. Wang, Z. H. Liu, *Angew. Chem. Int. Ed.* **2011**, *50*, 6851; d) C. H. Lu, H. H. Yang, C. L. Zhu, X. Chen, G. N. Chen, *Angew. Chem. Int. Ed.* **2009**, *48*, 4785.
[13] C. H. Lu, C. L. Zhu, J. Li, J. J. Liu, X. Chen, H. H. Yang, *Chem. Commun.* **2010**, *46*, 3116.
[14] Y. X. Jiang, X. H. Fang, C. L. Bai, *Anal. Chem.* **2004**, *76*, 5230.
[15] C. M. Chen, Q. H. Yang, Y. G. Yang, W. Lv, Y. F. Wen, P. X. Hou, M. Z. Wang, H. M. Cheng, *Adv. Mater.* **2009**, *21*, 3007.

Received: November 3, 2012
Revised: December 20, 2012
Published online: January 30, 2013

